

Combustion Stability Analysis of Composite Propellants with Octogen

Marica Bogosavljević¹⁾
Slavko Mijatov¹⁾
Aleksandar Milojković¹⁾
Vesna Rodić¹⁾

Research of operating pressure levels with irregular combustion and the effect on combustion instability of composite solid propellants with different quantity of octogen (HMX) are presented in this paper. The content of HMX increased in relation to the oxidant, ammonium perchlorate (AP). Combustion stability of the propellants was improved by adding titanium (IV) oxide powder and through the optimal projected ratio of two oxidizer fractions. Parameters of burning rate laws were determined and p-t diagrams were observed and compared.

Key words: Composite solid propellant, octogen, ballistic behaviour, combustion instability.

Introduction

THE beginning of nitramine propellants research is related to the concept of smokeless rocket propellants i.e. chlorine-free. By replacing double-base propellants with the composite ones, the problem of higher combustion temperatures also appears, and thus, the increased temperature load of the combustion chamber. This means that replacing the charge in standard metal components implied the composition of aluminium-free composite rocket propellants, providing a range increase of up to 20% compared with double-base propellants, but with higher combustion temperatures. This is why one of the possible solutions to aforementioned problems (smoke and temperature) has led to research in the field of nitramine propellants and replacement of a part of the ammonium perchlorate with HMX, RDX or CL-20, as the most representative and commonly used compounds [1].

The use of HMX (octogen, 1,3,5,7-tetranitro-1,3,5,7-tetraoctane) in composite rocket propellant compositions will be discussed in more detail in this part of the research, according to previously done research [2].

The aim of this research was not the observation of the composition parameters defined by the classical experiment plan, but the possibility of preparing the composition itself and its more reliable characterization. Consequently, these batches are only possible compositions and variants for establishing the two most important initial facts: casting time and combustion stability. The studies of nitramine composition presented here determine the applicability and influence of HMX on the castability and the occurrence of combustion instability.

The purpose of this research is to analyse the combustion of composite solid propellants composed of bimodal ammonium perchlorate powder and HMX crystals in a

polybutadiene binder, and whether these compositions can be applied as rocket propellants.

Theoretical part

Different raw materials and their ratios affect the characteristics that are important in creating the composition of any energetic material. The adjustment of certain properties often leads to the deterioration of others, which means that the design of the composition must be conducted with the aim of obtaining the optimum characteristics and fulfillment of as many requirements set for the propellant as possible. All raw constituents decompose, evaporate and/or combust, producing interacting gases as an energy flame by which the combustion process takes place [3].

Regular performances regarding burning rate law parameters are essential in creating the propellant composition. Smoke reduction is an additional requirement for concealing the trajectory of a projectile and position of a launcher, but also for reducing the amount of chlorine compounds and the negative impact on the environment. One of the possibilities for obtaining a composition with lower amounts of chlorine is to use nitramine compounds: high-energy and high-density materials producing high-temperature gaseous products, such as RDX (hexogen, 1,3,5 – Trinitro – 1,3,5 – triazine) and HMX (octogen, 1,3,5,7-tetranitro-1,3,5,7-tetraoctane). These have been considered as alternatives to ammonium perchlorate (AP) in composite rocket propellants (CRP) [4]. They are used with the aim of obtaining better energy performance at equivalent flame temperatures, as the propellant performance varies inversely with the molecular weight of the exhaust products.

However, the introduction of the nitramine components decreases the combustion stability of CRP, and due to the

larger molecule of the explosive component relative to the AP, the viscosity increases due to steric disturbances and better compatibility among organic components [2].

Therefore, before dealing with the energy characteristics, it is necessary to tackle the basic ones: castability, combustion stability and correction of combustion rates and pressure exponents. In order to produce a usable propellant formulation, it is necessary to control the burn rate of the propellant, to prevent unacceptable performance (too high or too low pressure) for the intended purpose of the device. The equation linking the burning rate parameters is shown in (1)

$$v = B \times p^n \quad (1)$$

where:

- v – burning rate,
- p – pressure in the motor chamber,
- B – const. depending on grain temperature and
- n – pressure exponent.

Preliminary studies regarding the castability and the ability to adjust combustion rates and pressure exponents of the compositions up to 25 wt.% of HMX were shown in the previous paper [2]. Research in this paper is related to the analysis of pressure levels that provide combustion stability of the compositions. Defining the usable compositions means controlling the appearance of the "hump" on the pressure diagrams due to the occurring instability.

Burning rates of CRP with HMX and RDX are usually much lower in comparison to propellants containing only AP, and in some cases, variations in particle size have minimal effect on the change of the burning rate [3]. Because of that, the particle packaging has a very important role.

In order to increase the burning rate, and avoid undesirable combustion instability of the propellant, additives such as Titanium (IV) oxide (TiO_2), can be useful, due to their ability to affect the combustion process [5,6,7].

The subject of this research, octogen, (HMX), is shown in Figures 1 and 2.

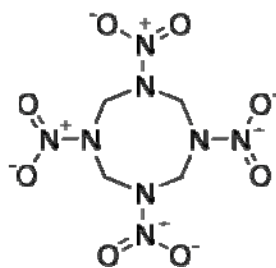


Figure 1. Structure of HMX

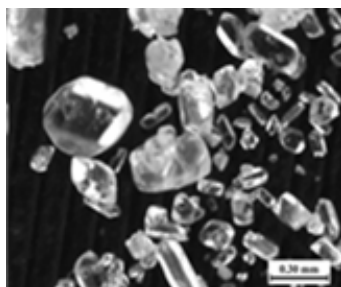


Figure 2 The crystals of HMX

Experimental part

The propellant binder matrix was based on hydroxyl-terminated polybutadiene (HTPB, R-45M, Arco) as prepolymer, isophorone-diisocyanate (IPDI), as curing agent

and dioctyl-adipate (DOA) as plasticizer, with other standard components. Titanium (IV) oxide was used as combustion stabilizer and burning rate modifier [2, 5].

Seven batches of propellant containing HMX were produced, as shown in Table 1, with a total energetic solid phase (AP + HMX) of 80 wt.%. During homogenization, and additional setting of the casting time due to reduced castability of compositions with higher HMX content (particle size $< 125 \mu\text{m}$ [8]), additional quantity of plasticizer was required in the last three batches (marked with "**"), as shown in Figures 3 and 4.

Table 1. Produced propellant compositions

No	AP (200/10) (wt.%)	AP _{tot} (wt.%)	HMX (wt.%)	TiO ₂ (wt.%)	DOA, (PHP**) (wt.%)
536	45.5/24.5	70	10	1.5	15
544	42.25/22.75	65	15	2	15
551	39/21	60	20	2	15
552	35.75/19.25	55	25	2.5	15
659*	32.5/17.5	50	30	2.5	20
660*	29.25/15.75	45	35	3	25
662*	26/14	40	40	3	35

** PHP (Parts per Hundred Parts) of polymer HTPB

The initially projected ratio of two oxidizer fractions was AP-200:AP-10=65:35, has shown to be the most favorable in previous studies. The amount of HMX was increased due to the decrease of oxidizer, while maintaining the given ratio of AP fractions and the total amount of the energy-solid phase.



Figure 3. Uncured propellant with a proper pot life



Figure 4. Unfavourable appearance of propellant

All ingredients were homogenized at 60 °C. The uncured propellant was cast in the chamber of experimental rocket motors (see Fig.5), used for static tests after the curing process in the oven at $(70 \pm 2)^\circ\text{C}$ for 5 days. After the loading of the test rocket motors, and changing the set of test motor chamber nozzles at 20°C, tests were conducted.



Figure 5. Casting of uncured propellant in the motor case

Behavior of CRP during casting was checked by sampling the uncured propellant after mixing process at $(60 \pm 2)^\circ\text{C}$ using Brookfield HBT viscometer [3].

Experimental results

Tests of viscosity value changes are presented in Table 2.

Table 2. Propellant viscosities of CRP/HMX propellants

No	Changes of viscosity values (Pa·s) during time (min)				
	15	30	45	60	75
536	160	188.8	220.8	251.2	288
544	176	236	280	312	352
551	182.4	238.4	276.8	318.4	360
552	264	368	419.2	494.4	-
659	227.2	260.8	280	296	321.6
660	281.6	368	408	432	449.6
662	422.4	468.8	-	512	520

The experimental results of burning rate law parameters at 20°C are given in Table 3: burning rate values at 70 bar (v_{70}), pressure exponents (n) and constant (B). These results were obtained by processing the $p=f(t)$ diagrams (pressure-operating time) for each nozzle diameter.

Table 3. Burning rate law parameters of CRP/HMX propellants at 20°C

No	v_{70} , [mm/s]	B	n
536	7.01	2.1783	0.2752
544	6.92	2.5469	0.2353
551	6.52	2.0384	0.2735
552	6.37	1.9062	0.2840
659	5.80	1.3598	0.3413
660	5.63	1.0802	0.3887
662	5.00	0.7332	0.4519

The $p=f(t)$ dependencies are shown in the next diagrams (Figures 6-12). The appearance of the "hump" on the pressure diagrams due to the occurring instability in the case of some compositions was noticed.

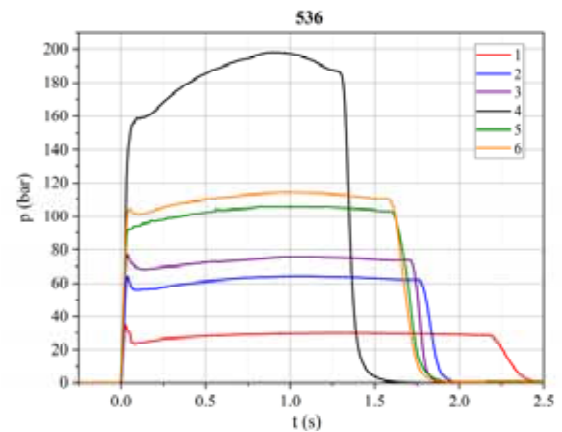


Figure 6. $p=f(t)$ dependencies of batch No 536

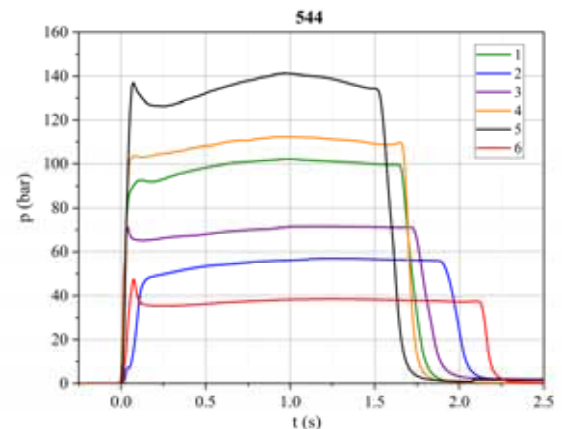


Figure 7. $p=f(t)$ dependencies of batch No 544

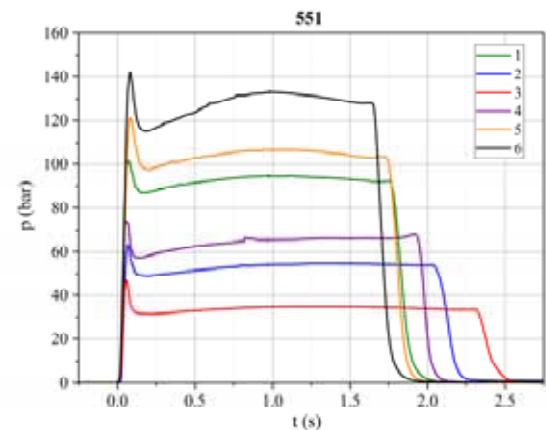


Figure 8. $p=f(t)$ dependencies of batch No 551

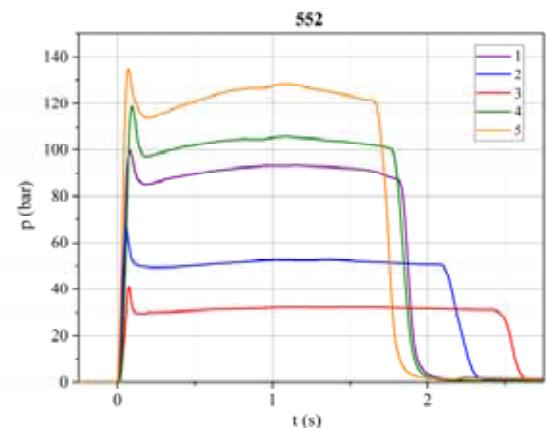


Figure 9. $p=f(t)$ dependencies of batch No 552

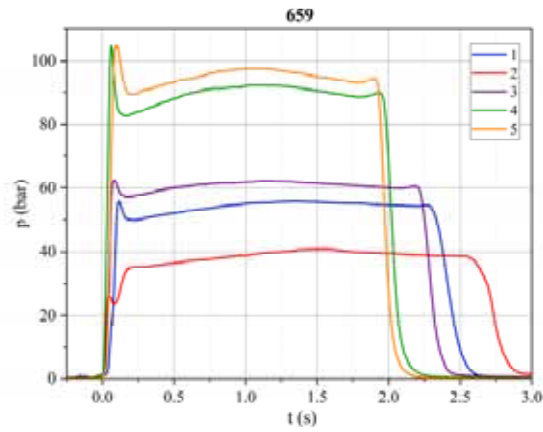


Figure 10. $p=f(t)$ dependencies of batch No 659

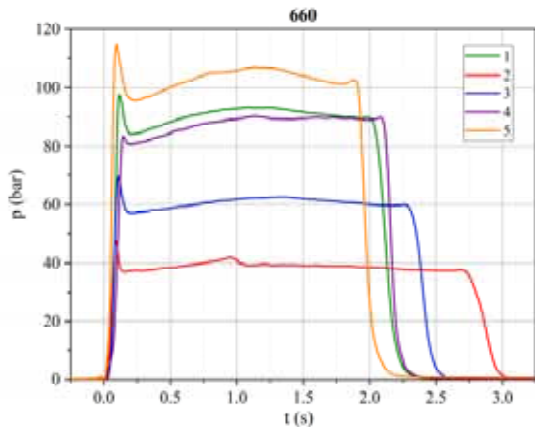


Figure 11. $p=f(t)$ dependencies of batch No 660

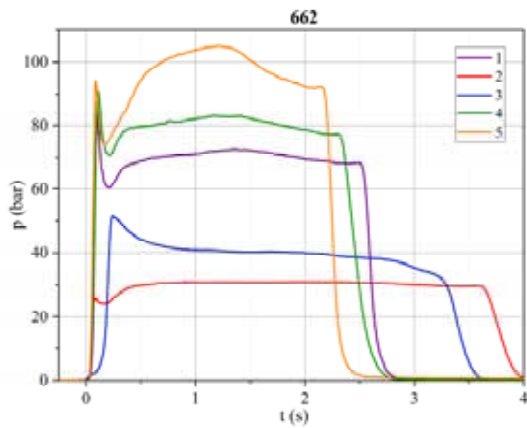


Figure 12. $p=f(t)$ dependencies of batch No 662

These diagrams were used for the calculation of the total impulse, operating time, mean and maximum pressure, for each dimension of nozzle (d_{cr}), and finally, the parameters of burning rate law given in Table 3. Based on these calculations, further conclusions were made.

Discussion

The aim of this research was to evaluate the quantity of HMX that could be incorporated into CRP, while observing the resulting parameters, with the possibility of adjusting the composition and obtaining useful and usable propellants depending on their purpose or requirements. The batches present possible compositions and variants for determining combustion stability range.

As it was previously noted [2, 9], it is difficult to regulate the parameters of the burning rate law with nitramine components in the CRP. The operating stable pressure is expected to decrease by increasing the amount of HMX. The levels of observed pressures are proportionate to [10]:

$$p_c \cong \left(\frac{A_b}{A_t} \right)^{\frac{1}{1-n}} \quad (2)$$

where p_c – chamber pressure, A_b – combustion area of propellant, A_t – cross-sectional nozzle area, n – pressure exponent in burning rate law.

As the ratio A_b/A_t is equal to the value K_N , (restriction coefficient), it could be said that:

$$p_c \propto K_N^{\frac{1}{1-n}} \quad (3)$$

Calculated values of mean pressures for each nozzle diameter and experimental grain measures, from the dependencies shown in Figs. 6-12 are given in Table 4. All groups of data are transformed in log-log system (see Fig. 13), and the parameters of $p_m=f(K_N)$ dependencies, as $y=a \cdot x^b$, (where $b=1/(1-n)$), are also shown in Table 4.

Table 4. Data pairs formed for $p=f(K_N)$

No	K_N	Pm (bar)	a	1/1- n	n*	R ²
536	234.35	29.10	0.0096	1.462	0.316	0.955
	387.28	62.52				
	526.15	73.78				
	626.53	110.56				
	758.65	185.55				
544	296.20	37.62	0.0084	1.470	0.320	0.962
	387.28	54.61				
	526.15	69.97				
	574.04	99.47				
	626.53	110.09				
551	296.20	34.03	0.0066	1.499	0.333	0.957
	387.28	53.39				
	526.15	65.00				
	574.04	93.32				
	626.53	105.06				
552	296.20	31.95	0.0044	1.566	0.361	0.998
	387.28	51.91				
	574.04	91.35				
	626.53	104.20				
	689.15	123.82				
659	387.28	38.16	0.0029	1.597	0.374	0.966
	449.45	54.13				
	543.83	62.30				
	626.53	91.17				
	689.15	96.41				
660	387.28	40.21	0.0075	1.439	0.305	0.995
	543.83	61.96				
	664.00	88.62				
	689.15	91.39				
	758.65	103.67				
662	387.28	30.33	0.0012	1.710	0.415	0.979
	581.98	70.58				
	689.15	80.86				
	758.65	96.43				

Calculated values a from Table 4, like those in Fig. 13, show that the lines shift towards lower pressures by increasing the HMX content in relation to the observed value of K_N . The slopes of the lines also increase, which means that the pressure values of the compositions with larger HMX content are more sensitive to changes in K_N . Likewise, the occurrence of instability for the same K_N value would happen at lower pressure [11].

Calculated pressure exponents, n^* (Table 4) correspond to the experimentally determined values (Table 3). All calculated pressure exponents are acceptable, and some changes in the amounts of TiO_2 could further improve the combustion process.

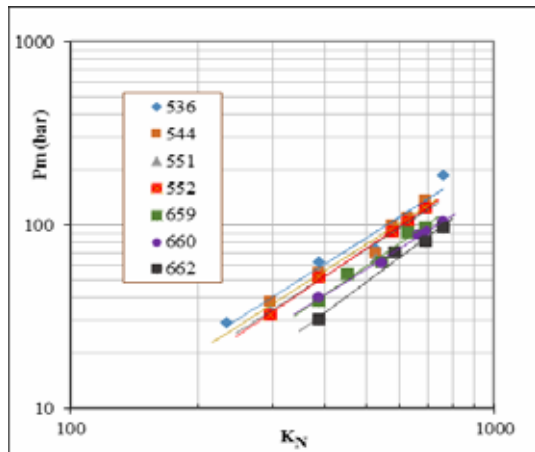


Figure 13. Summary representation of $pm=f(KN)$

In case that the content of HMX in CRP was observed, the following results were obtained (Fig. 14).

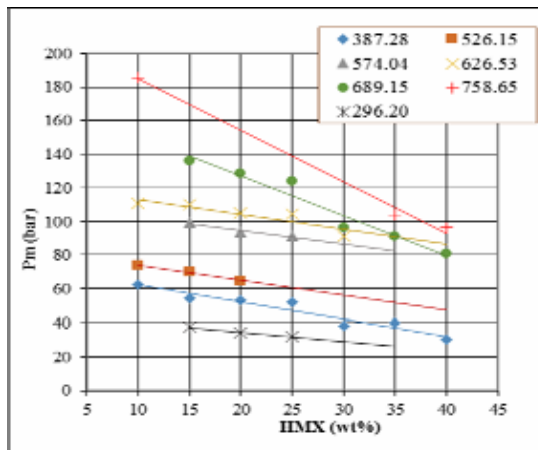


Figure 14. Summary representation $pm=f(HMX \text{ wt.}\%)$.

The parameters of linear curves ($y=ax+b$) from Fig. 14 are listed in Table 5.

Table 5. Parameters of fitted linear curves

d_{cr}	K_N	a	b	R^2
8.13	296.20	-0.5666	45.864	0.9765
7.11	387.28	-1.0043	72.413	0.9227
6.10	526.15	-0.8781	82.753	0.9941
5.84	574.04	-0.8117	110.94	0.9188
5.59	626.53	-0.8933	122.08	0.8123
5.33	689.15	-2.3687	174.64	0.948
5.08	758.65	-3.0691	215.51	0.9931

According to Fig.14, it could be concluded that all compositions have a stable burning rate of up to 100-110 bar.

However, the last two slopes show a significant deviation from the previous direction coefficient and a drop in the measuring pressure. Data for several higher values of K_N will be chosen and compared with the corresponding pressure level of compositions.

Corresponding data pairs (p_m vs. $HMX \text{ wt.}\%$) for four highest K_N values are given in Table 6.

Table 6. Data for obtained pressures for chosen K_N

K_N	536	544	551	552	659	660	662
574.04		99.47	93.32	91.35			
626.53	110.56	110.09	105.06	104.20	91.17		
689.15 ¹⁾		135.96	128.60	123.82			
689.15 ²⁾					96.41	91.39	80.86
689.15		135.96	128.60	123.82	96.41	91.39	80.86
758.65	185.55					103.67	96.43

¹⁾ 15 PPH DOA; ²⁾ 20, 25, 35 PPH DOA

Additional content of DOA in the last three batches, shifted the line along the y axis: the data pairs of linear curve for $K_N=689.15$ (as seen in the example) could be divided into two and extrapolated to the projected pressure values for lower and higher HMX wt.% (Fig. 15). It is clear that additional content of DOA contributes even more to the decrease in the pressure, which should be kept in mind for future research. Regardless, for this research, the mutual curve was used, because the added amount of DOA was necessary for the quality of the composition (see Fig.4).

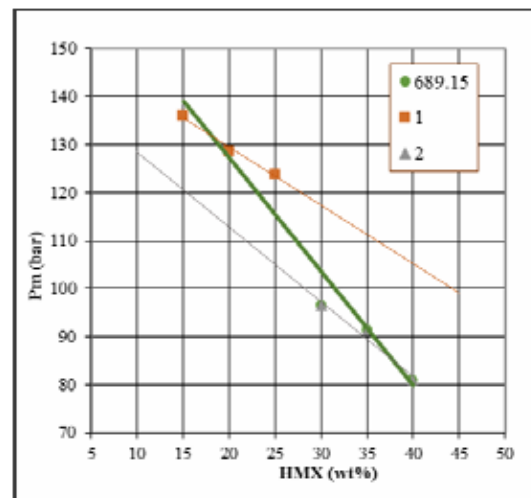


Figure 15. Explained case of $pm=f(HMX \text{ wt.}\%)$

For the considered CRP composition of 35 - 40 wt.% HMX, the limits of working pressure can be estimated from Fig.14: the range from 80 to 110 bar corresponds to two last lines and it could be the point of the evaluated limit of stable burning for defined nitramine propellant compositions.

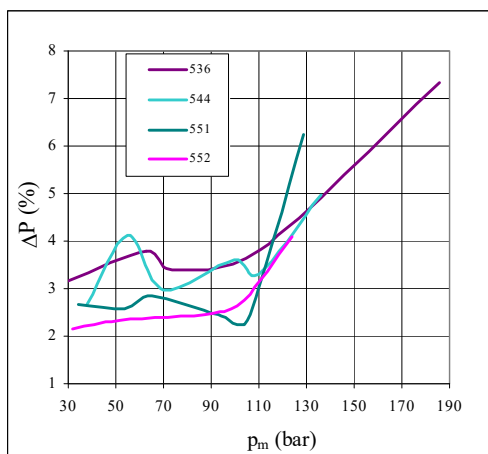
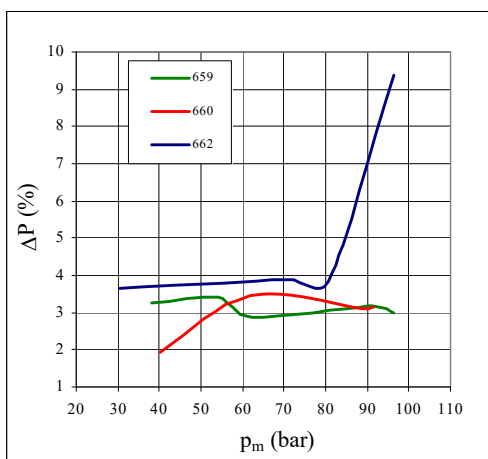
The diagram that shows the instability point of each composition is shown in Fig.16. It can be seen that an important value for consideration is the ratio between the difference of determined maximum pressure of operating range and calculated mean pressure value, and mean value itself (in percentages), Δp , for each K_N according to data from Figures 6-12. That would be the measure of the "humping" effect at working pressures.

Due to the very large number of data (for each composition and each K_N), not all obtained results are presented in this paper, but only the diagram and some characteristic data pairs (Table 7).

Table 7. Expression of „humping“ effect, Δp , (%)

K_N	387.28	526.15	574.04	626.53	689.15	758.65
No						
536	3.780	3.390		3.819		7.347
544	4.112	2.977	3.621	3.314	4.956	
551	2.571	2.842	2.464	2.335	6.246	
552	2.343		2.490	2.772	4.092	
659	3.277	3.398	2.887	3.167	3.001	
660	1.948	3.456		3.087	3.135	3.562
662	3.653		3.895		3.849	9.365

Two separate diagrams are shown in Figures 16 and 17, for a better overview.

**Figure 16.** The „humping“ effect in CRP (≤ 25 wt.% HMX)**Figure 17.** The „humping“ effect in CRP (30–40 wt.% HMX)

From the first diagram (Fig.16), it can be seen that the limits of stable burning amount to 170 bar (10 wt.% HMX) i.e. 130 bar (15–25 wt.% HMX). However, the limit for stable burning of CRP with 40 wt. % HMX falls down to 90 bar. Based on this, it can be concluded that the pressure limits for 30 and 35 wt.% HMX were not achieved for chosen parameters of K_N , but these values can be estimated between 90 and 130 bar.

Conclusion

Research presented in this paper provided useful data and applied analytical calculations which corresponds to potential ranges of stable burning of seven composite rocket propellants with 10–40 wt.% HMX and constant energetic

solid phase of 80 wt.% (octogen and bimodal mixture of ammonium-perchlorate, 200 μm and 7 μm in ratio 65/35). Binders were based on hydroxyl-terminated polybutadiene and isophorone diisocyanate, and TiO_2 was added as the combustion stabilizer. The aim was to evaluate the quantity of octogen that could be incorporated into CRP, and obtain useful and usable propellants depending on their purpose or requirements.

Using experimental rocket motors, the $p = f(t)$ diagrams (pressure-operating time) for each nozzle diameter and each prepared batch were obtained. Based on these data pairs, integrals of pressure, working times, maximum and mean pressures were calculated, as well as the parameters of burning rate law. The occurrence of the "hump" on some pressure diagrams is the consequence of the combustion instability. These increases in pressure are the consequence of the presence of a strong gas compression wave that propagates longitudinally through the internal cavity of the motor chamber.

Using the calculated values from $p=f(t)$ diagrams it was concluded that transformed linear dependencies shift towards lower pressures by increasing the HMX content in relation to K_N . Slopes of the lines indicate that the pressure values for compositions with larger HMX content are more sensitive to changes in K_N , so the occurrence of instability for the same K_N value would happen at lower pressure. Due to the decrease of castability of these compositions, additional amounts of plasticizer were added. Additional amount of DOA in the last three batches with 30, 35 and 40 wt.% HMX contributed even more to the decrease in pressure.

Based on these diagrams, it can be seen that the limits of stable burning amount to 170 bar (10 wt.% HMX) i.e. 130 bar (15–25 wt.% HMX). However, the limit for stable burning of CRP with 40 wt. % HMX falls down to 90 bar. Any change in the composition related to the solid phase results in the change of stable burning limits. All calculated pressure exponents from burning rate laws are acceptable, and some changes in the amounts of TiO_2 could further improve the combustion process.

References

- [1] Kalman J., Essel J. Influence of Particle Size on the Combustion of CL-20/HTPB Propellants, *Propellants Explos. Pyrotech.* 2017, 42, 1261–1267
- [2] Rodić, V. Bogosavljević, M. Milojković, A. Brzić, S. Fidanovski, B. Gligorijević, N. Preliminary Research of Composite Rocket Propellants Including Octogen, *Scientific Technical Review, Belgrade*, 2017., Vol. LXVII, No.1.
- [3] Beckstead, M. Recent Progress in Modeling Solid Propellant Combustion, *Combustion, Explosion and Shock Waves*, November 2006, Volume 42, Issue 6, pp 623–641
- [4] Ping Yin, Jiaheng Zhang, Lauren A. Mitchell, Damon A. Parrish, and JeanQne M. Shreeve *Angew. Chem.* 2016, 128, 13087–13089 T 2016 Wiley-VCH Verlag GmbH & Co. KGaA, Weinheim
- [5] Rodić, V. Dimić, M. Brzić, S. Gligorijević, N. Cast Composite Solid Propellants with Different Combustion Stabilizers, *Scientific Technical Review, Belgrade*, 2015., Vol. LXV, No.2.
- [6] Kubota, N. Combustion of Composite Propellants: Combustion of Composite Propellants, in *Propellants and Explosives, Thermochemical Aspects of Combustion*, Wiley-VCH Verlag GmbH & Co. KGaA, Weinheim, Germany. doi: 10.1002/9783527693481.ch7, 2015.
- [7] Lengellé, G. Duterque, J. Trubert, J.F. Combustion of Solid Propellants, RTO/VKI Special Course on "Internal Aerodynamics in Solid Rocket Propulsion", held in Rhode-Saint-Genèse, Belgium, 27-31 May 2002, and published in RTO-EN-023, pp 43-58
- [8] SORS 7572/97 Brizantni (sekundarni) Eksplozivni. Oktogen, Ciklotetrametenetranitramin, Odeljenje za standardizaciju, metrologiju i nomenklaturu u SMO, Savezno ministarstvo odbrane, Beograd, 1997.

- [9] Rodić, V. Bogosavljević, M. Milojković, A. Mijatov, S. Preliminary Research of Composite Rocket Propellants with Hexogen and Titanium Oxide Powder, Scientific Technical Review, Belgrade, 2018., Vol. LXVIII, No.2, pp. 36–47.
- [10] Rastogi, P. Singh, H.J. Deepak, D. Srivastava A.K., Pressure

dependence of burning rate of composite solid propellants, AIAA

Received: 15.07.2020.

Accepted: 01.09.2020.

Analiza stabilnosti sagorevanja kompozitnih raketnih goriva sa oktogenom

U ovom radu prikazano je istraživanje u oblasti sagorevanja čvrstog kompozitnog raketnog goriva sa različitim udelom oktogena (NMH) odnosno izvršena je analiza kako bi se utvrdilo pri kojem nivou radnog pritiska dolazi do pojave nepravilnog sagorevanja goriva i koji su njegovi efekti. Udeo NMH povećavan je u sastavu goriva u poređenju sa oksidatorom, amonijum-perhloratom (AR). Stabilnost sagorevanja raketnih goriva poboljšana je dodatkom titan(IV)-oksida u sastave uz održavanje optimalno definisanog odnosa dve frakcije korišćenog oksidatora. Određeni su parametri u zakonu brzine sagorevanja, p-t dijagrami su analizirani i međusobno poredeni.

Ključne reči: čvrsto kompozitno raketno gorivo, oktogen, balistika, nestabilnost sagorevanja